

## Effect of the $\text{NaVO}_3\text{-V}_2\text{O}_5$ Ratio on the High Temperature Corrosion of Chromium

J. Porcayo-Calderon<sup>1,\*</sup>, V.M. Salinas Bravo<sup>2</sup>, R.A. Rodriguez-Diaz<sup>3</sup>, L. Martinez-Gomez<sup>4,5</sup>

<sup>1</sup> Universidad Autonoma del Estado de Morelos, CIICAp, Av. Universidad 1001, 62209-Cuernavaca, Morelos, Mexico

<sup>2</sup> Instituto de Investigaciones Eléctricas, Reforma 113, Col. Palmira, C.P. 62490, Cuernavaca, Morelos, Mexico.

<sup>3</sup> Universidad Popular Autonoma del Estado de Puebla, A. C., 21 Sur No. 1103, Colonia Santiago, C. P. 72160, Puebla, Puebla, Mexico.

<sup>4</sup> Universidad Nacional Autonoma de Mexico, Instituto de Ciencias Fisicas, Av. Universidad s/n, Cuernavaca, Morelos, Mexico

<sup>5</sup> Corrosion y Proteccion, Buffon 46, Mexico City, C.P. 11590, Mexico

\*E-mail: [jporcayoc@gmail.com](mailto:jporcayoc@gmail.com)

*Received:* 12 February 2015 / *Accepted:* 29 March 2015 / *Published:* 28 April 2015

---

The effect of the  $\text{V}_2\text{O}_5\text{-NaVO}_3$  ratio on the corrosion resistance of Cr at different temperatures has been studied. The corrosion performance was determined by mass loss and electrochemical techniques. The corrosion resistance of Cr depends on the stability of the oxide layer grown, the testing temperature and the characteristics of the melt. Cr has good corrosion resistance up to 700 °C. Above 700 °C its corrosion resistance decreases since the solubility of the protective oxide formed increases. The corrosiveness of vanadium salts depends not only of its ability to absorb oxygen but also of the type of vanadium compound.

---

**Keywords:** Molten salts, polarization, weight loss, SEM, high temperature corrosion.

### 1. INTRODUCTION

In general the corrosion is the degradation of a material due to the oxidizing environment, and the corrosion degradation affects in a negative way the properties of the materials, which must be preserved to some applications. However there are particular types of materials degradation where the corrosion is carried out in an accelerated manner, for example the so-called molten salt corrosion. Molten salt corrosion is an accelerated degradation of a metal or alloy whose surface is covered by a

thin layer of molten salt at high temperature in an oxidant environment. Molten salt corrosion was first recognized as a serious problem in 1940 in connection with the degradations of the wall tubes of furnaces present in electrical plants, which generate vapor at high temperatures. Since then, the corrosion problem has been observed in furnaces, combustion machines, gas turbines, and waste to energy plants among others. Sodium sulphate ( $\text{Na}_2\text{SO}_4$ ) is one of the main species involved in molten salt corrosion, and it arises during combustion of fuel oils from the reaction between sulphur and sodium chloride. Both species can be found as impurities in the fuel and in the combustion air. Other particularly dangerous species in the molten salt corrosion process is vanadium, which also is found as an impurity in heavy fuel oils. During the combustion of this kind of fuels, some condensed phases like  $\text{Na}_2\text{SO}_4$ ,  $\text{V}_2\text{O}_5$  y  $\text{NaVO}_3$  can be formed. These compounds become very corrosive for the materials of energy conversion systems if they reach their melting point at the operating temperatures of the heat transfer surfaces where they deposit, as they induce metallic dissolution and accelerated oxidation at high temperature [1-12].

For catastrophic corrosion to occur, it is necessary the dissolution of the protective oxide layer. The solubility of the protective oxides in molten salts sulphate-vanadate mixture is higher than in  $\text{Na}_2\text{SO}_4$ . Several studies have been carried out in order to determine the corrosiveness of the  $\text{Na}_2\text{SO}_4$ - $\text{V}_2\text{O}_5$  mixtures, and it has been found that the highest corrosion rate occurs in the interval 10 a 30%  $\text{Na}_2\text{SO}_4$  [13]. Generally speaking, the corrosiveness of the different V-containing compounds depends upon its ability to absorb oxygen [13-14], and the highest corrosion rate and oxygen absorption experimented by the different vanadates is observed on those which have an atomic ratio of  $\text{V}/\text{Na} = 6$ , and the compound that best exemplifies this relationship is  $\text{Na}_2\text{O} \cdot \text{V}_2\text{O}_4 \cdot 5\text{V}_2\text{O}_5$ .

The presence of vanadium compounds makes very difficult for protective oxides to grow as dense, adherent and protective scales. Zhang and Rapp [15] have shown that vanadate ions increase the acidic fluxing of any oxide, consequently increase the acidic dissolution of any protective oxide. Acid-base reactions between vanadium molten salts and different oxides, qualitatively show that the corrosivity of the Na-V-O melts decreases with the acidity of the melt,  $\text{V}_2\text{O}_5 > \text{NaVO}_3 > \text{Na}_3\text{VO}_4$  [16]. On the other hand, it has been reported that the presence of the  $\beta$  (beta) and  $\gamma$  (gamma) sodium vanadil vanadates ( $\text{Na}_2\text{O} \cdot \text{V}_2\text{O}_4 \cdot 5\text{V}_2\text{O}_5$  and  $5\text{Na}_2\text{O} \cdot \text{V}_2\text{O}_4 \cdot 11\text{V}_2\text{O}_5$ , respectively) are the most aggressive vanadium compounds and they are responsible for the catastrophic corrosion in superheaters and reheaters of boilers burning heavy fossil fuels [1-2, 10, 13]. Since the aggressiveness of these complex vanadates depend on its oxygen absorption capacity, then it is possible that the degree of reactivity of the Na-V-O melts could be affected not only by the basicity of the melt, but also by oxygen absorption and temperature.

It is known that the corrosion resistance of a metal or alloy depends on the chemical stability of the protective oxide developed on its surface. However, in service conditions involving high temperatures a protective oxide should have good adhesion, low gas permeability, high thermodynamic stability, low diffusion coefficients, and low solubility in molten salts [16-20]. The main protective oxides with these characteristics are  $\text{Cr}_2\text{O}_3$ ,  $\text{Al}_2\text{O}_3$  and  $\text{SiO}_2$ .

However, because the corrosion performance of many of the alloys employed in high temperature applications is based on their ability to grow a protective layer of  $\text{Cr}_2\text{O}_3$ , is important to determine the effect of environmental variables (such as temperature, kind of vanadium compound,

basicity and oxygen absorption capacity) on the stability of this protective layer. Therefore, in this work a study was carried out in order to establish the effect of the  $\text{NaVO}_3\text{-V}_2\text{O}_5$  ratio on the high temperature corrosion process of pure Cr in the temperature span of 600 to 900 °C.

## 2. EXPERIMENTAL PROCEDURE

### 2.1. Sample Preparation

Pure chromium, 99.99%, was used for this research. Rectangular parallelepiped specimens of 10mm×5mm×5mm were cut down using a diamond tipped blade. Sample surfaces were grounded using silicon carbide sandpaper. Grinding process began with 120-grit sandpaper until all major scratches and burs were removed. The process was continued with 220, 400, and 600-grit sandpaper until all surfaces were uniform. Once the grinding was complete, samples were washed with distilled water then by ethanol in an ultrasonic bath for 10 minutes before the tests.

### 2.2. Vanadium Compound

The vanadium compound used included sodium metavanadate  $\text{NaVO}_3$ ,  $2\text{NaVO}_3\text{:}5\text{V}_2\text{O}_5$  mixture (which allows the formation of sodium  $\beta$ -vanadil-vanadate,  $\text{Na}_2\text{O}\cdot\text{V}_2\text{O}_4\cdot5\text{V}_2\text{O}_5$ ),  $10\text{NaVO}_3\text{:}7\text{V}_2\text{O}_5$  mixture (which allows the formation of sodium  $\gamma$ -vanadil-vanadate,  $5\text{Na}_2\text{O}\cdot\text{V}_2\text{O}_4\cdot11\text{V}_2\text{O}_5$ ) and vanadium pentoxide ( $\text{V}_2\text{O}_5$ ). Where the highest basicity corresponds to  $\text{NaVO}_3$ , the highest oxygen absorption capacity corresponds to  $10\text{NaVO}_3\text{:}7\text{V}_2\text{O}_5$  mixture, and the highest acidity corresponds to  $\text{V}_2\text{O}_5$ . Both the pure compounds and salts mixture were ground into an agate mortar. This was done so that all salts have the same grain size and to homogenize the salts mixture.

For simplicity, hereafter we will use the following nomenclature: V =  $\text{V}_2\text{O}_5$ , NV =  $\text{NaVO}_3$ , NV6 =  $2\text{NaVO}_3\text{:}5\text{V}_2\text{O}_5$  or  $\text{Na}_2\text{O}\cdot\text{V}_2\text{O}_4\cdot5\text{V}_2\text{O}_5$ , and NV3 =  $10\text{NaVO}_3\text{:}7\text{V}_2\text{O}_5$  or  $5\text{Na}_2\text{O}\cdot\text{V}_2\text{O}_4\cdot11\text{V}_2\text{O}_5$ , with N =  $\text{Na}_2\text{O}$ . Where the melting point of compounds formed are 691 °C, 630 °C, 627 °C and 535 °C, respectively [2, 21].

### 2.3. Mass Loss Tests

Before corrosion tests, the specimens were cleaned with acetone and dried and then packed in the mixture of salts in porcelain crucibles with 500 mg/cm<sup>2</sup> of vanadium salt. The corrosion tests were carried out in electric furnaces in a static air during 100 hours at temperatures of 600, 700, 800 and 900 °C. Four specimens were exposed to each test condition. After corrosion tests the corrosion rate was measured as mass loss. Three specimens of each condition test were decaled and chemically cleaned according to ASTM G1 standard, and other specimen was mounted in thermosetting resin in cross-section and polished to analyze the subsurface corrosive attack using a Karl Zeiss DSM-950 scanning electronic microscope (SEM) with an X-ray energy dispersive (EDS) analyzer.

#### 2.4. Electrochemical Tests

Electrochemical experiments were performed using an ACM Instrument controlled by a personal computer. A typical three electrode arrangement was used with two platinum wires as pseudo-reference electrode and counter electrode. All the potentials described in the text are relative to the platinum electrode, unless stated differently. For electrical connection of the working electrode a Ni20Cr wire was spot welded. Ceramic tubes were used for isolating the electrical wire from the molten salt, the gap between the ceramic tube and electrical connection wire was filled with refractory cement. Size, preparation of specimens and corrosive mixtures were the same for electrochemical tests. Owing to the melting point of the salts, the test temperatures were 700, 800 and 900 °C. A 20 ml alumina crucible was used for containing the corrosive mixture and placed inside an electrical furnace. When the test temperature was stabilized, the three electrochemical cell electrodes were introduced inside the molten salt. In all experiments, the atmosphere above the melt was static air. Experimental setup used in the present study is shown in Figure 1.

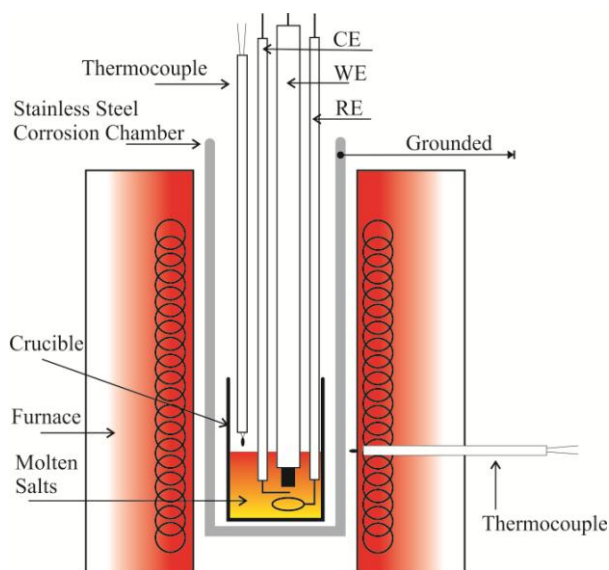


**Figure 1.** Experimental setup of the electrochemical cell.

One of the main problems of the electrochemical techniques used in molten salt corrosion at high temperatures has been the use of a correct reference electrode. The most commonly used reference electrode is an Ag wire immersed in molten salt which contains  $\text{Ag}^+$  ions; such salt with  $\text{Ag}^+$  ions is separated from the study system by a conductive membrane [22]. The second option as reference electrode is a platinum wire (Pt) submerged in molten salt which has  $\text{Pt}^+$  ions at a specific molar concentration [23]; both options are isolated from the studied electrochemical medium by a membrane [23-24]. However, the conductive membranes used are not commercial, therefore it is necessary to manufacture them in the laboratory. For this reason, in this study, the conductive membrane was not created, and instead a formal reference electrode was used, which met three conditions: constant potential, a well-known redox couple and fast kinetic, i.e., a pseudo-reference

electrode was used. This pseudo-electrode was a Pt immersed directly in electrolytic medium for corrosion evaluation, however the redox electrochemical couple was not identified, and it has not been reported [6-8, 10-12, 25-30]. However, in order to check if the pseudo-reference electrode was stable, another platinum electrode was immersed in the working salts and the potential of the first electrode was monitored with time once the temperature was stabilized (900 °C). This potential at the beginning was 25 mV nobler than the second platinum electrode, but after 45 min this difference was very stable, having a fluctuation of  $\pm 3$  mV. Sidky and Hocking that other well-established facts for the choice of Pt as the pseudo-reference electrode are not only its reversibility and unpolarizability in the selected salt media, but also its stability and reproducibility [25]. Recently Kasen and Jones [31] investigated the usefulness of platinum (melting point; 1768.3 °C) as an electrochemical reference electrode and they concluded that under certain conditions, such as high temperature or in molten electrolytes, where the usual reference electrodes such as calomel or Ag/AgCl/KCl electrodes cannot be used in electrochemical measurements, Pt is the reference electrode of choice.

For each measurement carried out, the linear polarization resistance (LPR), and the polarization curves ( $E_{corr}$  vs.  $I_{corr}$ ) were obtained. In order to determine LPR, a potential polarization of  $\pm 10$  mV was applied and the variation in current intensity associated with that polarization was measured hourly up to a total of 24 hr. Tafel slopes ( $b_a$ ,  $b_c$ ) were obtained from the active regions of the corresponding anodic and cathodic curves by scanning the potential from -300 to 300 mV applying a scanning rate of 1 mV/s. From LPR measurements  $I_{corr}$  values were obtained using Stern-Geary equation.

$$I_{corr} = \frac{b_a b_c}{2.303 R_p (b_c - b_a)} \quad (1)$$

After testing, corroded specimens were mounted in thermosetting resin and examined in a Karl Zeiss DSM-950 scanning electronic microscope (SEM) with an X-ray energy dispersive (EDX) analyzer.

### 3. RESULTS AND DISCUSSION

#### 3.1. Polarization curves

Figures 2 to 4 show the results of potentiodynamic polarization curves for Cr in vanadium salts at 700, 800 and 900 °C, respectively. The polarization curves at different test temperatures displayed similar behavior. In general, it is observed that the addition of V modified the behavior of both the anodic and cathodic branches and the  $E_{corr}$  values. In all cases, the  $E_{corr}$  value was displaced in the anodic direction, and this displacement was based on the V ratio in the melt. The  $E_{corr}$  gap was higher when V content was higher. It is observed that the magnitude of this gap decreases with increasing temperature. At 800 °C a significant variation in  $E_{corr}$  values is not observed in NV3, NV6 and V. Similarly it is observed an increase in the  $I_{corr}$  value (one order of magnitude) with the addition of V

respect to the value observed in NV. Similar behavior has been noted by other authors in molten sulfates where the addition of  $V_2O_5$  in small amounts increases the  $I_{corr}$  values until two orders of magnitude [32]. This increase in the aggressiveness of the melt is due to the acid character of  $V_2O_5$ , which increases both the melt acidity and the solubility of the protective oxides [33].

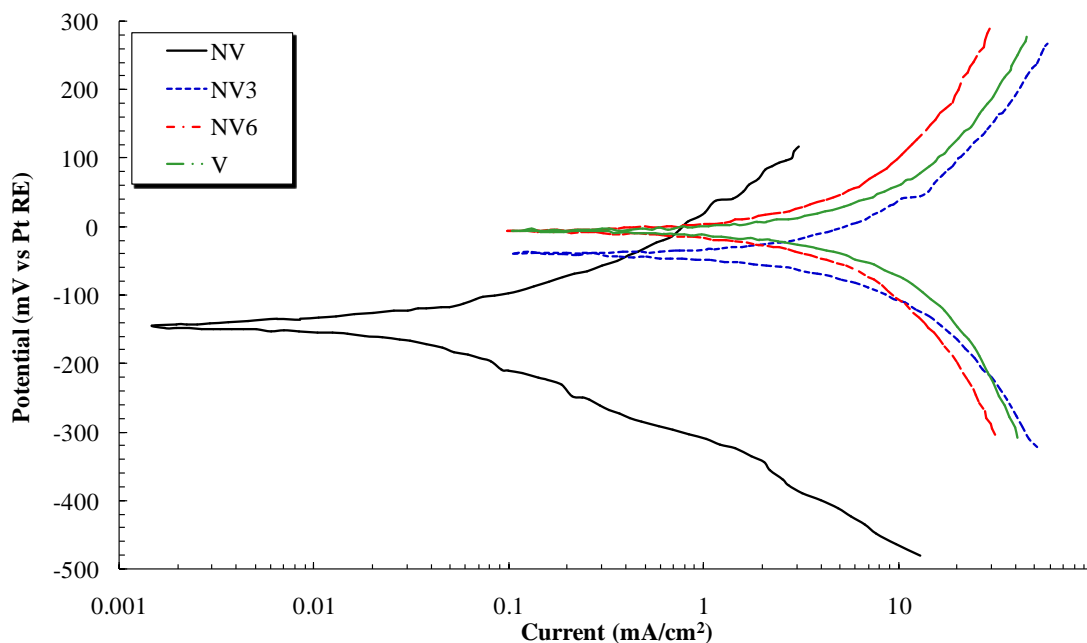


**Figure 2.** Potentiodynamic polarization curves for Cr in different NV-V ratio at 700 °C.

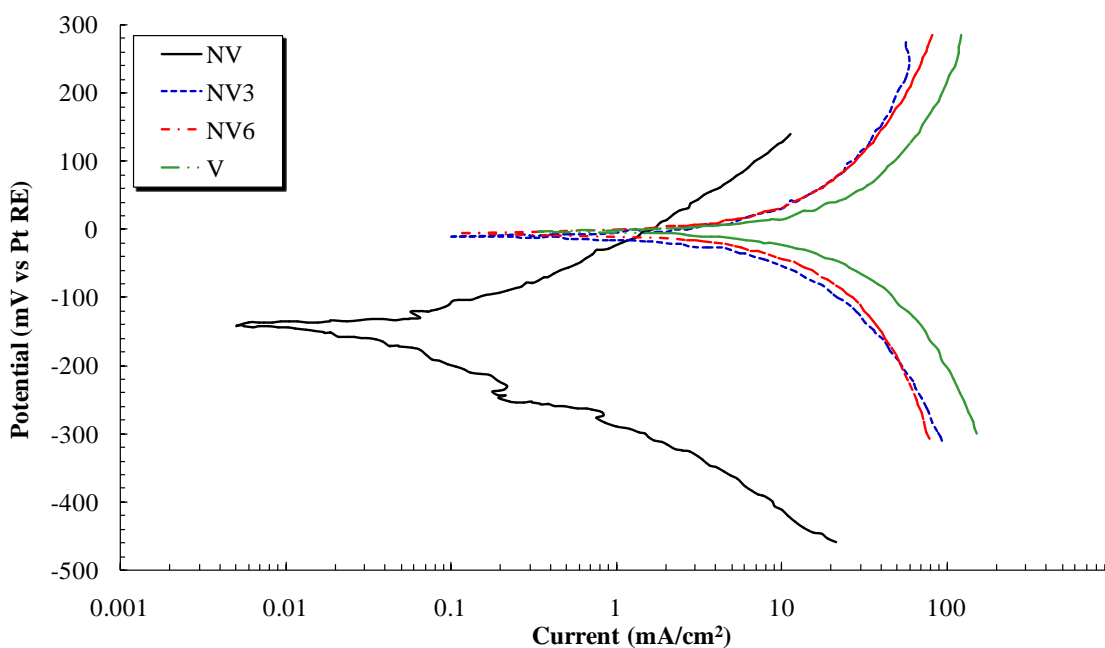


**Figure 3.** Potentiodynamic polarization curves for Cr in different NV-V ratio at 800 °C.

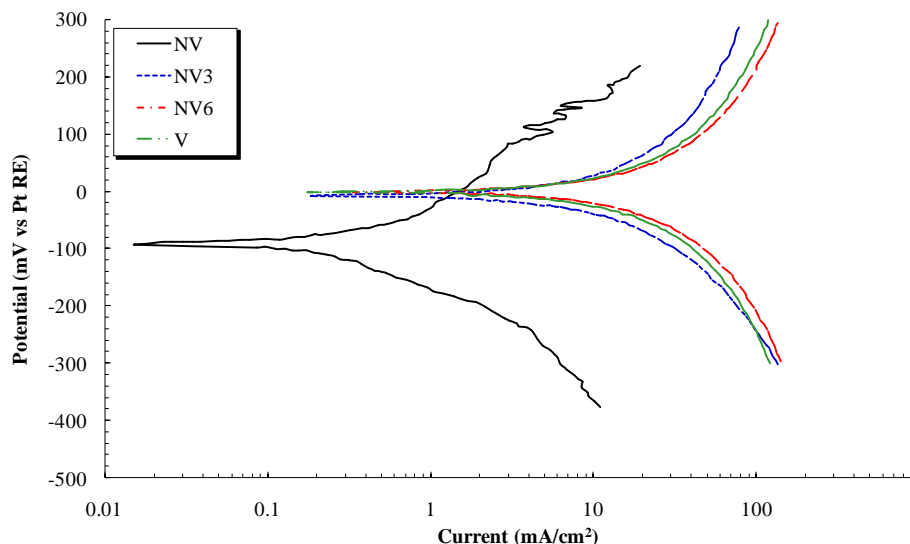


**Figure 4.** Potentiodynamic polarization for Cr in different NV-V ratio at 900°C.

The V addition modified the behavior of the cathodic branch increasing its slope in relation to the quantity of V present in the melt. Similar trends have been reported and this is attributed to occurrence of diffusion controlled reactions at the electrode interfaces [32, 34-36]. Since vanadium is a transition element it can exist in various oxidation states, being +5 and +4 the most stable valence states. The  $V^{5+}$  and  $V^{4+}$  ratio depends on the oxygen partial pressure and and/or its basicity. The presence of these multivalent metallic ions in a molten salt increases the corrosion rate due to the counter-diffusion of multivalent cations or electron hopping, which would provide rapid transport of charge through the melt [33]. Cyclic voltammetric studies [32] have showed that the presence of  $V_2O_5$  in the melts increase the current considerably high, and that the process responsible for this can be due to the formation of different types of vanadate ions in its  $V^{5+}$ ,  $V^{4+}$  and  $V^{3+}$  states.

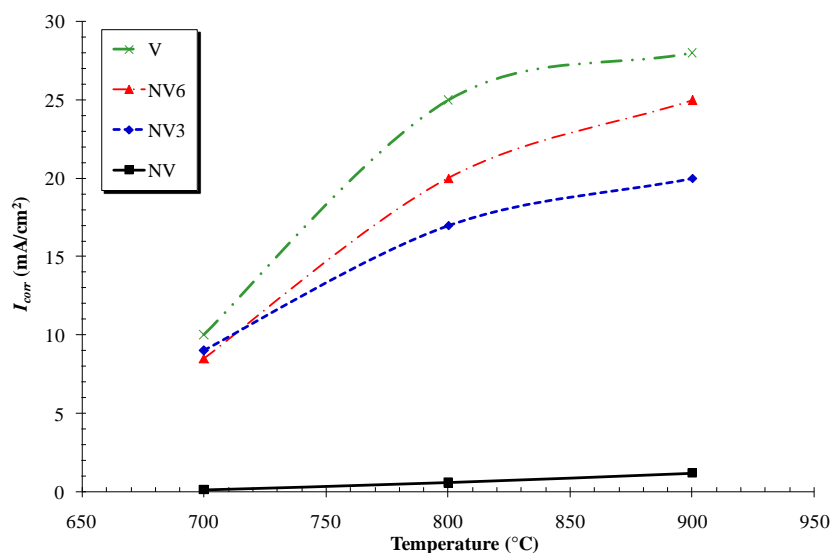
In all cases, the behavior of the anodic branches show a continuous increase in current without showing any limiting current, indicating that the anodic processes is the determining factor for corrosion in the presence of vanadium salts. However, in the case of melts with V addition, this increment is greater (one order of magnitude) and is also affected by temperature. The behavior of the anodic and cathodic branches denote that the strong ability of vanadium to reduce its lower oxidation states is the main cause that enhances the Cr corrosion in the vanadate melts. This is explained because vanadium acts as an electron sink in the molten salt system and consume electrons released by oxidizing components of the system [32]. In addition, Mittelstadt and Schwerdfeger [37] indicate that the presence of  $Na_2O$  stabilizes the highest oxidation state of vanadium, and therefore the  $I_{corr}$  values also varied according to the  $Na_2O$  content of in molten salts ( $NV < NV3 < NV6 < V$ ).

Figure 4 shows the  $I_{corr}$  change determined from the polarization curves for each NV-V ratio and test temperature. According to the figure, it is observed that the lower and highest corrosion rate was in the NV and V melts at all temperatures, respectively. In particular at 700 °C is observed that NV3, NV6 compounds show almost the same aggressiveness, and in this case both compounds have the highest oxygen absorbing capacity [13-14]. However, from 800 °C upwards there is a clearer

definition of the tendency of aggressiveness and this increase is in the order  $V > NV6 > NV3 > NV$ . This behavior is not a function of the oxygen absorption capacity, on the contrary depends of the melt acidity, i.e., the corrosion rate increases with the content of  $V_2O_5$ . This is consistent with studies indicating that the reactivity of some oxides in molten vanadates increase in the order  $V_2O_5 > NaVO_3 > Na_3VO_4$  [33]. It should be noted that the polarization tests can be considered as a pattern of the beginning of the corrosion process of the molten salt-alloy system, and this trend may change in long-term exposures.

### 3.2. Linear Polarization Resistance

Figures 6 to 8 show the  $I_{corr}$  variation with time from linear polarization tests of Cr in the different vanadium salts from 700 to 900 °C. It is noted that at 700 °C (Figure 6), chromium showed the highest corrosion rates to the first minutes of immersion in the molten salts, and subsequently they decreased to a nearly constant trend. This behavior may be due to the rapid development of a protective oxide layer [1-2, 10]. The initial behavior is in agreement with the  $I_{corr}$  measurements observed from polarization tests. At 800 °C (Figure 7) is observed a similar behavior to that shown at 700 °C, except that the  $I_{corr}$  values are higher as expected in a processes activated by temperature. At 900 °C (Figure 8) the higher corrosion rates were observed, and a gradual decrease in corrosion rate is not observed as that shown at 700 and 800 °C. This may be because it was not possible the grown and establishment of stable protective oxide, since this one was constantly dissolved by the vanadium salts [1-2]. These short time tests showed that in all cases the molten salts aggressiveness was a function of its acidity, i.e., its content of V, where the aggressiveness varied according to  $V > NV6 > NV3 > NV$ . The behaviors observed at all temperatures, show a uniform corrosion process because sudden changes in  $I_{corr}$  values were not observed. These trends can change for longer exposure times since a stability zone by the grown oxide is not observed [11-12].



**Figure 5.** Effect of temperature on the  $I_{corr}$  values at different NV-V ratio.

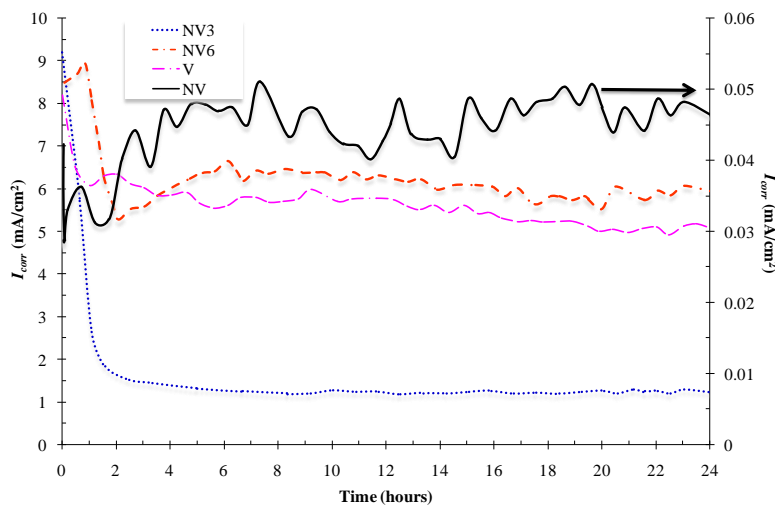


**Figure 6.**  $I_{corr}$  variation versus time for Cr in NV, NV3, NV6 and V melts at 700 °C.

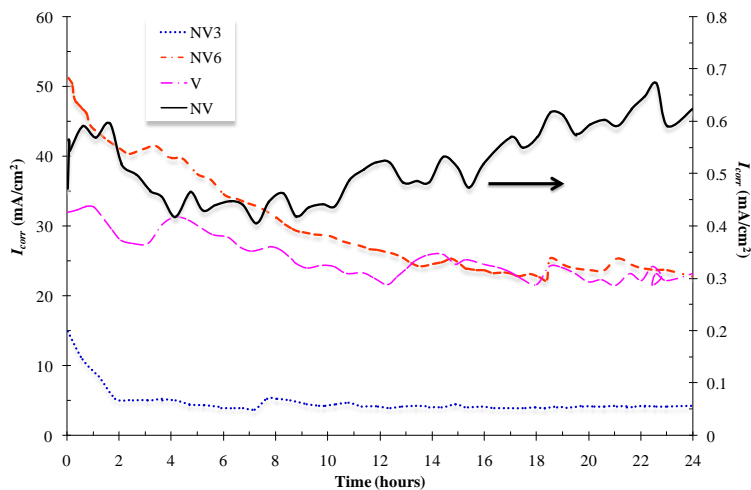


**Figure 7.**  $I_{corr}$  variation versus time for Cr in NV, NV3, NV6 and V melts at 800 °C.

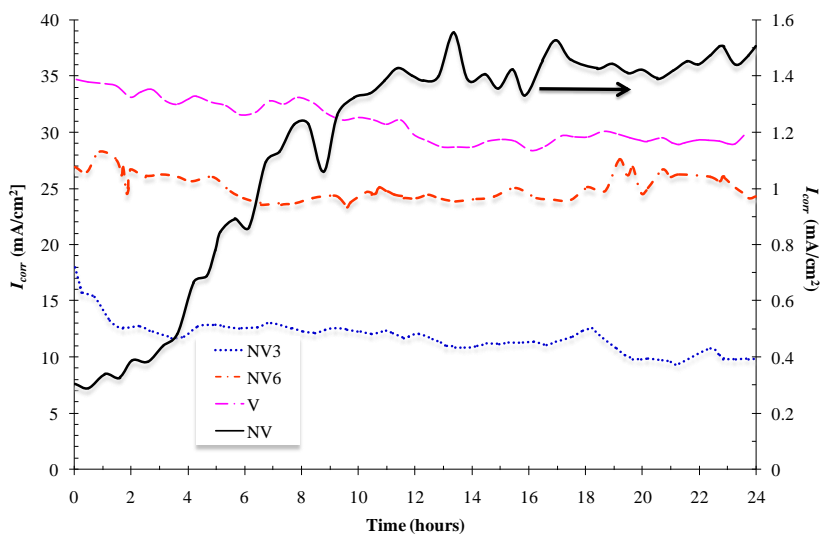


**Figure 8.**  $I_{corr}$  variation versus time for Cr in NV, NV3, NV6 and V melts at 900 °C.

### 3.3. Mass Loss Tests

In this case the mass loss tests were carried out from 600 to 900 °C for 100 hours, Figure 9 shows the results where the effect of the different salts on the corrosion rate is shown. From the figure it can be seen that at 600 and 700 °C the Cr corrosion rate is highest in NV3 and NV6 followed by NV and V, i.e., the aggressiveness of the molten salt was greater in those compounds with higher oxygen absorption capacity [13-14, 20, 38-39]. At 800 °C there is a clear separation of the corrosive behavior of the vanadium salts, and at 900 °C catastrophic corrosion rate values were observed, where the most aggressive compound was V, whereas the least aggressive compound was NV. At 800 and 900 °C it was observed that the aggressiveness of the molten salts was dependent on the vanadium contents;  $V > NV6 > NV3 > NV$ . From these results it can be considered that in vanadium molten salts, the stability of the protective oxide ( $Cr_2O_3$ ) is determined by three factors; the oxygen absorption capacity [13-14], salt acidity [33], and temperature.

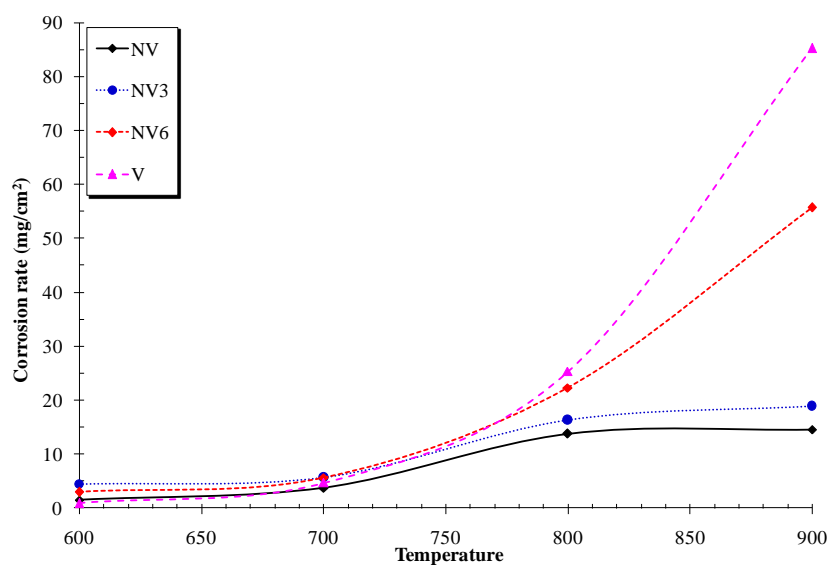


**Figure 9.** Corrosion rate for Cr in NV, NV3, NV6 and V as a function of temperature. Corrosion test of 100 hours.

Figures 10 throughout 13 show the SEM images of the cross section aspect of the Cr specimens after being exposed to the vanadium salts at 600, 700, 800 and 900 °C for 100 hours. According to Figures 9 and 10, it can be seen that the highest degradation and corrosion rate of Cr in NV was at 800 °C and 900 °C. Also, it shows that at all temperatures, an external three layer structure was observed, the first one was chromium oxide ( $Cr_2O_3$ ), the second one was a chromium vanadate layer, and the external layer was NV as identified by X-ray diffraction studies. It is evident that the oxide layer was dense and porous free, and the vanadate layer is thin.

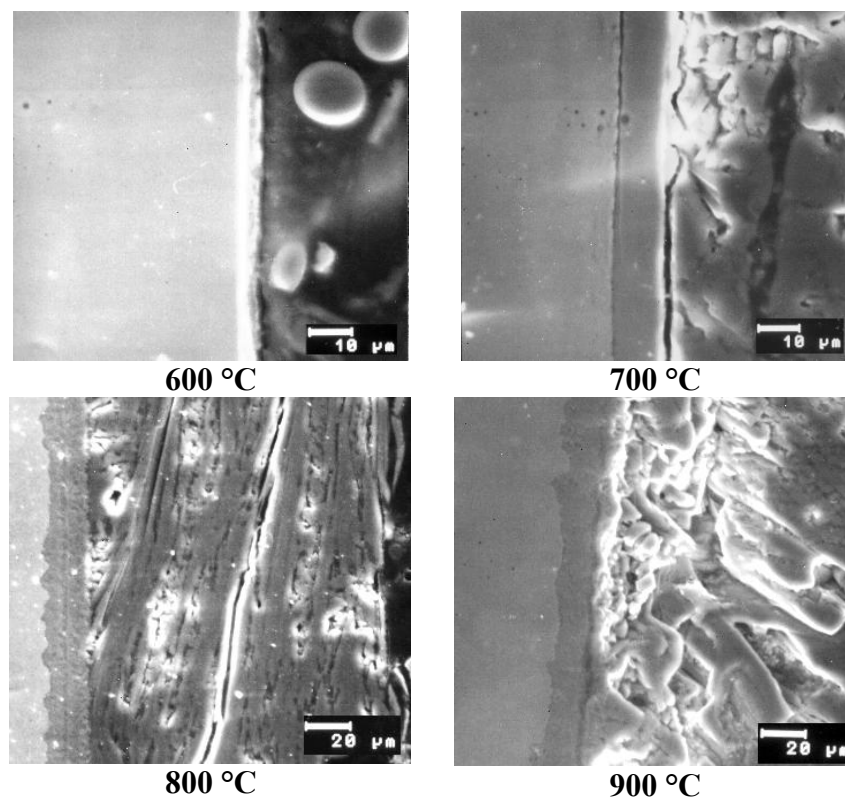


**Figure 10.** Cross section aspect for Cr after the corrosion test in NV at 600, 700, 800 and 900 °C for 100 hours.

Figure 11 shows micrographs of the cross sections of Cr exposed to NV<sub>3</sub>. This figure shows the presence of a protective oxide layer at 600 and 700 °C together with an external chromium vanadate layer. At 700 °C the protectiveness of the external oxide decreases which is evident by an increase in the corrosion rate at 800 °C (Figure 9) due to the oxide dissolution process by molten salts. From 800 to 900 °C, there is not a remarkable increase in the corrosion rate, and the micrographs show the presence of a thin oxide layer and a thick chromium vanadate layer together with the reprecipitation of chromium oxide particles. In this case, the chromium vanadate layer could have performed as a barrier against the penetration of the corrosive agent. However, notwithstanding that there is no substantial increase in the corrosion rate of chromium it is evident that chromium oxide is completely destroyed at temperatures higher than 800 °C. This is important because the corrosion rate in vanadium molten salts is determined by the stability of both protective oxide layer and corrosion products formed on the metallic surface, and consequently the stability of both is determined by temperature. For example, at temperatures where a solid corrosion products are formed at the metal surface, they can protect the metal even in the presence of molten phases. In this case, the corrosion rate is determined by the thickness and porosity of the corrosion products scale. A constant thickness is reached when the scale growth rate is equal to its removal rate by dissolution, as it could be observed in the case of NV (Figure 10). At temperatures where stable solid products are not formed, the integrity of the material is compromised because the formation rate of the protective oxide is lower than its dissolution rate. In engineering alloys this can result in a catastrophic corrosion process because the

continuous fluxing of the protective oxides may cause a bulk alloy depletion, and the new layer oxides formed can be less and less protective [1-2].

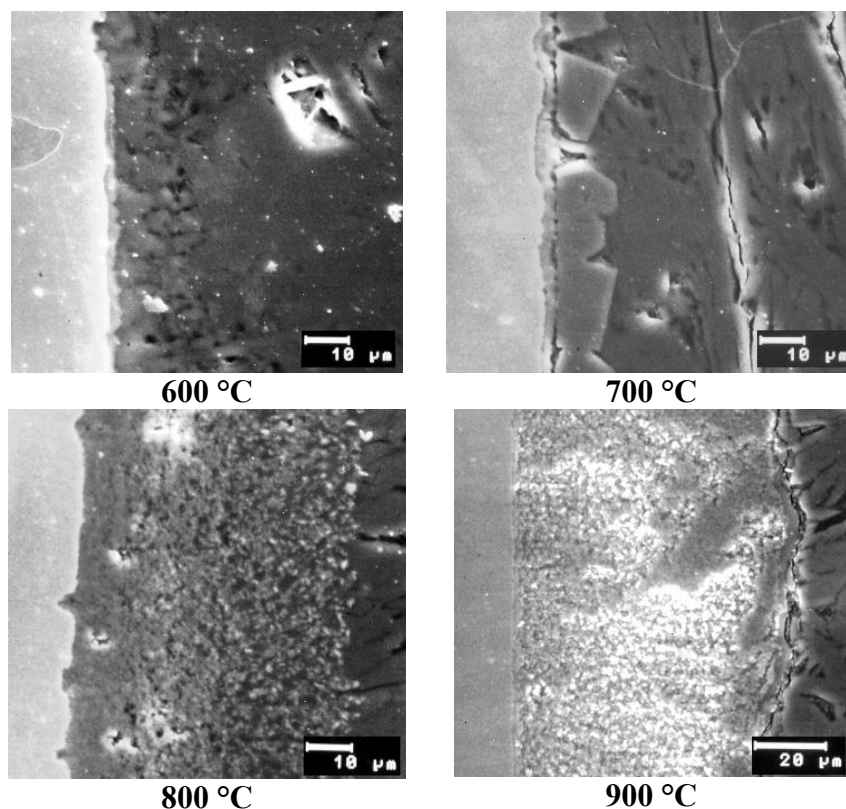


**Figure 11.** Cross section aspect for Cr after the corrosion test in NV3 at 600, 700, 800 and 900 °C for 100 hours.

Figure 12 shows the SEM images micrographs of the cross sections of Cr exposed to NV6. The presence of a protective oxide layer at 600 and 700 °C is observed. At 600 °C the presence of a corrosion product layer between the protective oxide and the vanadium salt was not observed; however, at 700 °C the presence of a chromium vanadate layer and a thin layer (~1 micron) of chromium oxide was found. At 800 and 900 °C the formation of a protective oxide layer was not found. Figure 13 shows the appearance in cross section of Cr evaluated at 900 °C in NV6 and the elements mapping for V and Cr. Figure shows the presence of a thick layer of corrosion products (Cr and V), and the absence of a layer of  $\text{Cr}_2\text{O}_3$ . According to the X-ray mappings, it could be seen that the chromium oxides were dissolved by the vanadium salts forming a porous layer of chromium vanadates allowing the precipitation of chromium oxide particles. In the case of the corrosion of chromium in NV6 as observed in Figure 9, the corrosion rate increases substantially depending on the temperature, in contrast to what was observed with NV and NV3, i.e., by increasing the acid nature of the molten salt (vanadium content) the chromium oxides are less protective.

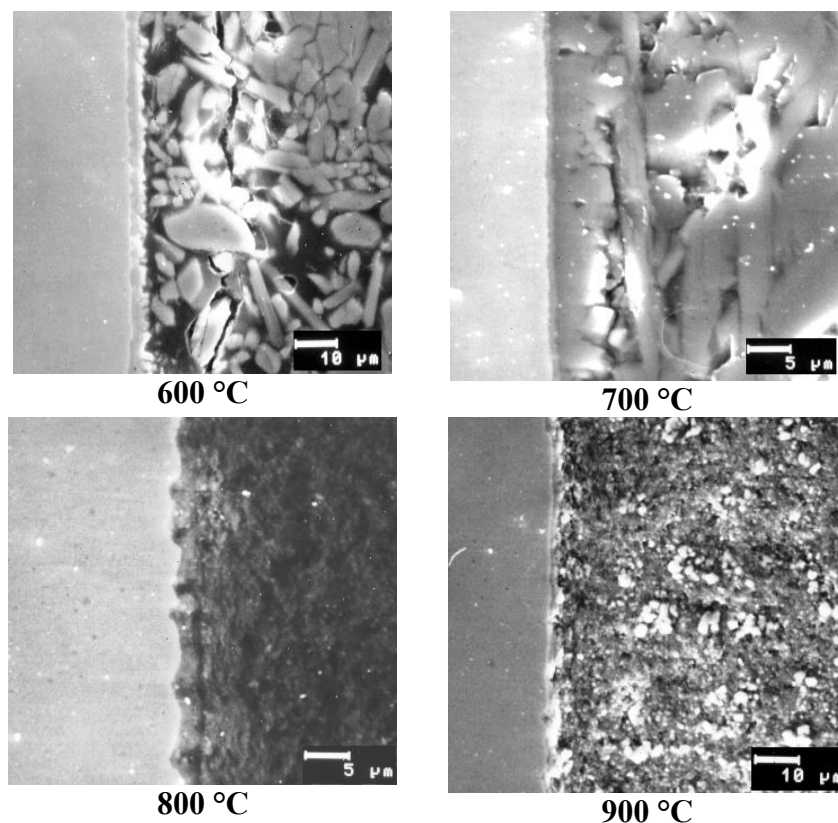


**Figure 12.** Cross section aspect for Cr after the corrosion test in NV6 at 600, 700, 800 and 900 °C for 100 hours.

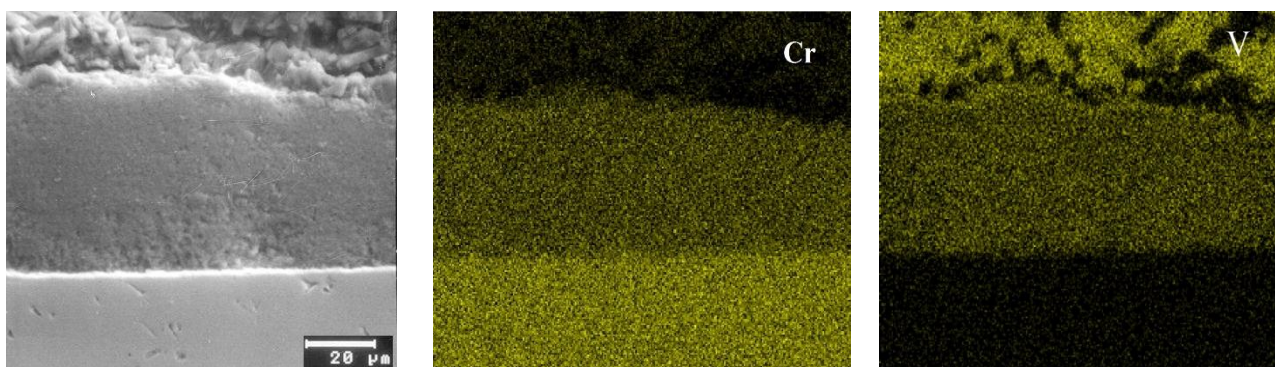


**Figure 13.** Aspect of Cr evaluated in NV6 at 900 °C and mapping of elements for Cr and V.

Figure 14 shows micrographs of the cross sections of Cr exposed to V. This figure shows that at 600 °C, chromium degradation is almost the same as that obtained in static air at the same temperature. Since the melting point of the salt is 690 °C, at 700 °C degradation increased slightly. This is substantiated by the thin oxide layer and the vanadate scale observed onto the Cr surface. At higher temperatures degradation increases rapidly (Figure 8 and 13). At 800 °C a fine chromium oxide layer and a thick one of chromium vanadate was observed (~80-100 micron). The corrosion rate was

increased significantly at 900 °C, due to the oxide dissolution, since a layer of porous oxide was observed. It was also found the presence of few particles of chromium vanadates.

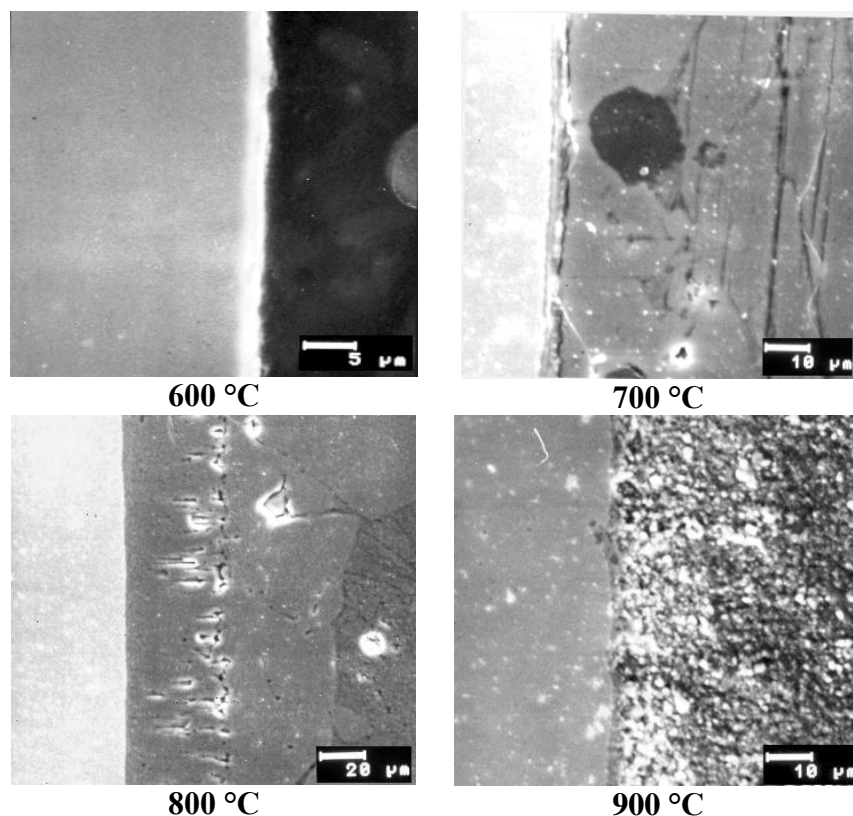
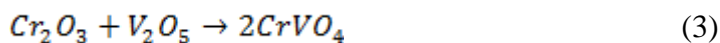
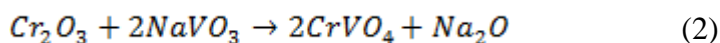


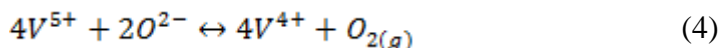
**Figure 14.** Cross section aspect for Cr after the corrosion test in V at 600, 700, 800 and 900 °C for 100 hours.

X-ray diffraction analysis performed on the corrosion products showed the presence of both  $\text{Cr}_2\text{O}_3$  and  $\text{CrVO}_4$ , except in the case of V at 600 °C where only chromium oxide was detected. Although at 600 °C only the NV3 was in a liquid state, the presence of the chromium vanadate in NV and NV6 was due to solid state reactions. These results demonstrate that the vanadium salts prevent the growth of dense and adherent protective oxides; in addition, Zhang and Rapp [15] have shown that the vanadate ions increase the acidic solubility of any oxide.

Then, considering that the only compounds present in the molten salts were the  $\text{NaVO}_3$  and/or  $\text{V}_2\text{O}_5$ , then the metallic vanadate detected could have been formed according with any of the following reactions:



Both reactions justify the aggressiveness shown by the vanadium salts. Particularly, low aggressiveness observed in NV can be due to the fact that during the reaction with the  $\text{Cr}_2\text{O}_3$ , besides forming the  $\text{CrVO}_4$  also  $\text{Na}_2\text{O}$  is formed. Where  $\text{Na}_2\text{O}$  decreases the acidity of the melt and stabilizes the higher oxidation state of vanadium ( $\text{V}^{5+}$ ) [37] thus decreasing the  $\text{V}^{5+}/\text{V}^{4+}$  proportion. The presence of these multivalent metallic ions increases the corrosion rate by providing a rapid transport of charge through the melt [33]. Similar effect has been reported by increasing the oxygen partial pressure [40-41]. The concentration of  $\text{V}^{4+}$  ions in the liquid state is dependent on the oxygen partial pressure above the melt, as shown below:



Decreasing oxygen partial pressure will lead to an increased  $\text{V}^{4+}$  ion concentration, with a corresponding increase in electrical conduction and a decrease in the corrosivity of the melt. Therefore one solution proposed for vanadate-induced corrosion by heavy oils in boilers is the use of low excess air. In this case,  $\text{NaVO}_3$  is the predominant species, consequently the metavanadate solute ion  $\text{VO}_3^-$  complexes with the oxide ions provided by the acidic dissolution of  $\text{Cr}_2\text{O}_3$  to form orthovanadate ion  $\text{VO}_4^{3-}$ . According to Rapp [42] the complexing reaction does not depend upon which oxide is providing the oxide ions, so that reaction is considered to be completely general for every oxide [43-52].

On the contrary, reaction 3 describes the aggressiveness of the melt only in the presence of V. In this case, the formation of the chromium vanadate does not generate by-products that modify the aggressiveness of the melt, unless the oxygen partial pressure is modified according to reaction 4. According to some authors, [40-41], electrical conduction in liquid vanadium pentoxide is considered to occur with electrons hopping from  $\text{V}^{4+}$  to  $\text{V}^{5+}$  centers by a thermally activated diffusion mechanism, at oxygen partial pressures greater than 0.1 atm. At lower pressures the conduction occurs by collective-electron conduction in partially filled 3d bands where the valence and conduction bands can be overlapped due to the cations separation in the melt becoming less than some critical distance, 0.297 nm.

However, the aggressiveness of NV6 and NV3 depends of both reactions. With a greater proportion of V, the melt aggressiveness is increased, ie, the effect of the  $\text{Na}_2\text{O}$  is inhibited due to the acidic nature of the V. Moreover these mixtures have the capability to accommodate a great amount of oxygen in the melt and the ability for a fast diffusion of oxygen through its layer to the metal surface. In vanadate mixtures there is an increase in the oxidizing character of the melt due to the presence of the redox couple ( $\text{V}^{5+}/\text{V}^{4+}$ ), and an increase in the ionic conductivity as a result of rapid oxygen exchange between the different vanadium oxide species, which favors oxide transport across the salt film [53]. Furthermore, according to Pantony and Vase [54] the protective action is normally related to poor conductivity of oxide films and in the presence of molten vanadates the rate of exchange with molecular oxygen is greater for those with higher electrical conductivity, therefore, involves also an enhanced diffusivity of oxygen and a consequent increase in the corrosive properties of the melt. Therefore, the highest corrosion rates observed in the melts with V it is due to the acid/base nature of

this oxyanion salt that enhanced the dissolution (fluxing) of the normally protective oxide scale, promoting the formation of a non-protective precipitated oxide particles in the corrosion products.

#### 4. CONCLUSIONS

The intensity of the degradation of chromium in vanadium salts depends on the nature of the oxide formed, temperature and corrosive agent. Chromium had an acceptable corrosion resistance up to 700 °C. However, above this temperature, its protective ability decreases due to an increase on the oxide dissolution in vanadium salts. The aggressiveness of vanadium salts is a function of temperature. The salts which induced highest corrosion rates on the temperature limit of 600 to 700 °C were NV3 and NV6, whereas at higher temperatures the highest corrosion rates were obtained in V. As temperature increases, the aggressiveness not only depends on the salt ability to absorb oxygen, but also of the vanadium content.

#### ACKNOWLEDGEMENTS

Financial support from Consejo Nacional de Ciencia y Tecnología (CONACYT, México) (Project 198687) is gratefully acknowledged.

#### References

1. A. Wong, R.I. Marchan, L. Martinez, *CORROSION/95*, Paper 465, (Houston TX: NACE Intl. 1995).
2. A. Wong-Moreno, Y. Mujica, L. Martinez, *CORROSION/94*, paper 185, (Houston, TX: NACE Intl. 1994).
3. J. Porcayo-Calderon, S. D'Granda, L. Martínez, *Materials Performance*, 34 (1995) 32-37.
4. J. Porcayo-Calderon, J.G. Gonzalez-Rodriguez, L. Martinez, *Journal of Materials Engineering and Performance*, 7 (1998) 79-87.
5. A. Martinez-Villafañe, M.F. Almeraya-Calderon, C. Gaona-Tiburcio, J.G. Gonzalez-Rodriguez, J. Porcayo-Calderon, *Journal of Materials Engineering and Performance*, 7 (1998) 108-113.
6. L. Martinez, M. Amaya, J. Porcayo-Calderon, E. Lavernia, *Material Science and Engineering A*, 258 (1998) 306-312.
7. M. Amaya, M.A. Espinosa-Medina, J. Porcayo-Calderon, L. Martinez, J.G. Gonzalez-Rodriguez, *Materials Science and Engineering A*, 349 (2003) 12-19.
8. V.M. Salinas-Bravo, J. Porcayo-Calderon, T. Romero-Castañon, G. Domínguez-Patiño, J.G. Gonzalez-Rodriguez, *Materials and Corrosion*, 56 (2005) 481-484.
9. V.M. Salinas-Bravo, J. Porcayo-Calderon, J.G. Gonzalez-Rodriguez, *Russian Journal of Electrochemistry*, 42 (2006) 560-565.
10. J.G. Gonzalez-Rodriguez, S. Haro, A. Martinez-Villafañe, V.M. Salinas-Bravo, J. Porcayo-Calderon, *Materials Science and Engineering A*, 435-436 (2006) 258-265.
11. O. Sotelo-Mazon, C. Cuevas-Arteaga, J. Porcayo-Calderon, V. M. Salinas-Bravo, G. Izquierdo-Montalvo, *Advances in Materials Science and Engineering*, Volume 2014, Article ID 923271, 12 pages, (2014), <http://dx.doi.org/10.1155/2014/923271>.
12. O. Sotelo-Mazón, J. Porcayo-Calderon, C. Cuevas-Arteaga, J. J. Ramos-Hernandez, J. A. Ascencio-Gutierrez, L. Martinez-Gomez, *Journal of Spectroscopy*, vol. 2014, Article ID 949168, 10 pages, 2014, <http://dx.doi.org/10.1155/2014/949168>.
13. G.W. Cunningham and A. de S. Brasunas, *Corrosion*, 12 (1956) 389t-405t.

14. N.D. Phillips and C.L. Wagoner, *Corrosion*, 17 (1961) 396t-400t.
15. Y.S. Zhang and R.A. Rapp, *Corrosion*, 43 (1987) 348-352.
16. R.A. Rapp, Hot corrosion of materials, in Selected Topics in High Temperature Chemistry, Eds. O. Johannesen and A.G. Andersen, Amst., Oxford, N.Y., Tokio: Elsevier, (1989), pp 291-329.
17. W.J. Quadackers, M.J. Bennet, *Materials Science and Technology*, 10 (1994) 126-131.
18. I. Wolf, H.J. Grabke, P. Schmidt, *Oxidation of Metals*, 29 (1988) 289-306.
19. H.W. Grunling, R. Bauer, *Thin Solids Films*, 95 (1982) 3-20.
20. J.R. Wilson, *CORROSION/76*, Paper 12, NACE International, Houston, Tx, USA, 1976.
21. Steam/its generation and use. 41st edition, editors: John B. Kitto and Steven C. Stultz. The Babcock & Wilcox Company, Barberton, Ohio, USA, 2005.
22. C.A.C. Sequeira, Fundamentals of Molten Salt Corrosion, C.A.C. Sequeira (Ed.), High Temperature Corrosion in Molten Salts in Molten Salt Forum, Trans Tech Publications Ltd., United Kingdom (2003), pp. 3-40.
23. H.A. Laitinen, C.H. Liu, *J. Am. Chem. Soc.*, 80 (1958), 1015.
24. H.A. Laitinen, J.W. Pankey, *J. Am. Chem. Soc.*, 81 (1959) 1053.
25. P.S. Sidky and M.G. Hocking, *Corrosion Science*, 27 (1987) 499-530.
26. J.I. Barraza-Fierro, M.A. Espinosa-Medina, M. Hernandez-Hernandez, H.B. Liu, E. Sosa-Hernandez, *Corrosion Science*, 59 (2012) 119-126.
27. J.G. Gonzalez-Rodriguez, A. Luna-Ramirez, M. Salazar, J. Porcayo-Calderon, G. Rosas, A. Martinez-Villafañe, *Mat. Sci. Eng.*, A399 (2005) 344-350.
28. G. Gao, F.H. Stott, J.L. Dawson, D.M. Farrell, *Oxidation of Metals*, 33 (1990) 79-94.
29. E. Otero, A. Pardo, M.C. Merino, M.V. Utrilla, M.D. Lopez, and J.L. del Peso, *Oxidation of Metals*, 51 (1999) 507-525.
30. E. Mohammadi Zahrani, A.M. Alfantazi, *Corrosion Science*, 65 (2012) 340-359
31. K.K. Kasem, S. Jones, *Platinum Metals Rev.*, 52 (2008) 100-106.
32. I.B. Singh, *Corrosion Science*, 45 (2003) 2285-2292.
33. Y.S. Hwang and R.A. Rapp, *Corrosion*, 45 (1989) 933-937.
34. A. Rahmel, M. Schmidt, and M. Schorr, *Oxidation of Metals*, 18 (1982) 195-223.
35. D.Z. Shi, J.C. Nava, and R.A. Rapp, *High Temperature Materials Chemistry IV*, (Electrochemical Soc.) USA, 1987, pp 1-25.
36. M. Amaya, J. Porcayo-Calderon and L. Martinez, *Corrosion*, 57 (2001), 489-496.
37. R. Mittelstadt, K. Schwerdfeger, *Metallurgical Transactions B*, 21B (1990) 111-120.
38. N.J.H. Small, H. Strawson, A. Lewis, in *International Conference on the Mechanism of Corrosion by Fuel Impurities*, L. M. Wyatt and G. J. Evans (Eds.), (Butterworths Marchwood, England, may 1963), pp 238-253.
39. W.J. Greenert, *Corrosion*, 18 (1962) 57t-67t.
40. R.C. Kerby, J.R. Wilson, *Canadian Journal of Chemistry*, 50 (1972) 2865-2870.
41. E. Chassagneux and G. Thomas, *Materials Chemistry and Physics*, 17 (1987) 273-284.
42. R.A. Rapp, *Corrosion Science*, 44 (2002) 209-221.
43. P. Mohan, T. Patterson, V.H. Desai, Y.H. Sohn, *Surface & Coatings Technology*, 203 (2008) 427-431.
44. T.S. Sidhu, S. Prakash, R.D. Agrawal, *Acta Materialia*, 54 (2006) 773-784.
45. D. Deb, S. Ramakrishna Iyer and V.M. Radhakrishnan, *Scripta Materialia*, 35 (1996) 947-952.
46. X. Chen, Y. Zhao, L. Gu, B. Zou, Y. Wang, X. Cao, *Corrosion Science*, 53 (2011) 2335-2343.
47. Sa Li, Zhan-Guo Liu, Jia-Hu Ouyang, *Corrosion Science*, 52 (2010) 3568-3572.
48. A. Keyvani, M. Saremi, M. Heydarzadeh Sohi, *Journal of Alloys and Compounds*, 506 (2010) 103-108.
49. Z. Xu, L. He, R. Mu, S. He, G. Huang, X. Cao, *Surface & Coatings Technology*, 204 (2010) 3652-3661.

50. Gosipathala Sreedhar, M.D. Masroor Alam, V.S. Raja, *Surface & Coatings Technology*, 204 (2009) 291-299.
51. Felicia M. Pitek, Carlos G. Levi, *Surface & Coatings Technology*, 201 (2007) 6044–6050.
52. C. Batista, A. Portinha, R.M. Ribeiro, V. Teixeira, C.R. Oliveira, *Surface & Coatings Technology*, 200 (2006) 6783–6791.
53. E. Rocca, L. Aranda, M. Moliere, P. Steinmetz, *Journal of Materials Chemistry*, 12 (2002) 3766-3772.
54. D.A. Pantony, K.I. Vasu, *J. Inorg. Nucl. Chem.*, 30 (1968) 755-779.

© 2015 The Authors. Published by ESG ([www.electrochemsci.org](http://www.electrochemsci.org)). This article is an open access article distributed under the terms and conditions of the Creative Commons Attribution license (<http://creativecommons.org/licenses/by/4.0/>).